Supplementary Information (SI) for Journal of Materials Chemistry C.


# Charge carrier dynamics modulation of $Ag_xInS_2$ thin films for high-performance photodetection

*Zhenglin Jia[1,2], Yuke Zhao[1,2], and Qianqian Lin[1,2,3,*]*

[1] Key Lab of Artificial Micro- and Nano-Structures of Ministry of Education of China, School of Physics and Technology, Wuhan University, Wuhan, 430072, China.

[2] Wuhan University Shenzhen Research Institute, Shenzhen 518057, China.

[3] Micius Laboratory, Henan Academy of Sciences, Zhengzhou 450001, China.

[*]Correspondence: q.lin@whu.edu.cn (Q.L.)

## 1. Experimental details

### 1.1 Materials

Silver nitrate ($AgNO_3$, 99.8%) was purchased from Chengdu Chron Chemicals. Bismuth nitrate pentahydrate ($Bi(NO_3)_3 \cdot 5H_2O$, 98.0%) was purchased from Sigma Aldrich. Indium chloride ($InCl_3$, 99.99%) was purchased from Aladdin. Thiourea (TU, 99%) and Stannic oxide ($SnO_2$, 15% in water) were purchased from Alfa Aesar. Acetonitrile (ACN, 99.5%) was purchased from Sinopharm Chemical Reagent Co., Ltd. 2, 2', 7, 7'-tetrakis (N, N-dipmethoxyphenylamine)-9, 9-spirobifluorene (Spiro-OMeTAD, 99.86%) was purchased from Liaoning Youxuan Technology Co., Ltd. Lithium bis(trifluoromethanesulphonyl)imide (Li-TFSI, 99%) was purchased from J&K Scientific. 4-tert-butylyridine (t-BP, 96%) and 2-Methoxyethanol (2-MOE, 99%) were purchased from Aladdin. Chlorobenzene (CB, 99.8%) and Lithium fluoride (LiF, 99%) were purchased from Sigma Aldrich. Molybdenum trioxide ($MoO_3$, 99%) was purchased from Macklin. All commercial products were used as received.

### 1.2 Fabrication of chalcogenide thin films via solution process:

#### 1.2.1 $Ag_xInS_2$ thin films

$Ag_xInS_2$ (x=0.8, 0.9, 1.0, 1.1, 1.2) precursor solution (0.5 M) with different Ag contents was obtained by mixing 135.89 mg, 152.88 mg, 169.87 mg, 186.86 mg or 203.84 mg $AgNO_3$, 221.18 mg $InCl_3$, 228.36 mg TU and 2 mL 2-MOE, stirring until fully dissolved at room temperature. This solution is colorless and transparent.

The $Ag_xInS_2$ thin films were prepared by spin-coating the solution on the substrates which has been cleaned at 3,000 RPM for 60 s. Then, the $AgInS_2$ films were annealed at a low temperature of 100℃ for 60 min and a high temperature of 320℃ for 10 min in glovebox with nitrogen atmosphere.

### 1.3 Device fabrication

Indium tin oxide (ITO)-coated glass was patterned with 100 μm channels by a high power (80 W) 1064 nm nanosecond pulse laser. Then, ITO-coated glass was sprayed with detergent and gently brushed clean with a toothbrush, followed by sonication, in turn, with deionized water and ethanol for 15 min each. The substrates were dried with

an air-gun and treated with UV-ozone before depositing thin films. Finally, various $Ag_xInS_2$ films were deposited by spin-coating of precursors.

Indium tin oxide (ITO)-coated glass substrates were sprayed with detergent and then gently cleaned with a brush, followed by sonication, in turn, with deionized water and ethanol for 20 min each. The substrates were then dried using an air gun powered by compressed air and treated with UV-ozone for 20 min before depositing thin films layer-by-layer according to the device structure: ITO/$SnO_2$/$Ag_xInS_2$/Spiro-OMeTAD/$MoO_x$/Ag/LiF/Ag. The $SnO_2$ layer was obtained by spin coating Water-dispersible solution of $SnO_2$ quantum dots (dilute in deionized water at a ratio of 1:3) at 4,000 RPM for 30 s and then wipe the edges with deionized water to expose the electrode portion, followed by a thermal annealing process on a hot plate at 150 °C for 30 min in ambient air atmosphere. Before depositing the absorption layer, the prepared $SnO_2$ thin films were exposed to ozone treatment for 20 min. Then, the $Ag_xInS_2$ film was obtained by spin-coating on the top of the $SnO_2$ layer, and the specific procedure was the same as the films fabricated. Spiro-OMeTAD layer was fabricated by spin-coating the doped spiro-OMeTAD solution on the top of $Ag_xInS_2$ films at 3,000 RPM for 60 s. The doped spiro-OMeTAD solution was prepared by dissolving 1mL CB solution of spiro-OMeTAD (72.3 mg/mL), 17.5 μL ACN solution of Li-TESI (520 mg/mL) and 29 μL t-BP and stirring for 4 hours. Finally, 8 nm $MoO_3$, 30 nm Ag, 60 nm LiF and 30 nm Ag were sequentially deposited on the top of the spiro-OMeTAD layers by thermal evaporation with metal masks.

### 1.4 Characterization

The surface morphology of chalcogenide thin films was obtained with a Zeiss GeminiSEM 500 Field Emission Scanning Electron Microscope. The absorption spectra were tested with an UV-Vis-IR spectrophotometer (PerkinElmer LAMBDA 1050). The Raman spectra were characterized with a Confocal Raman Microscope (XploRA Plus). The $J-V$ characteristics and photocurrent under illumination of the devices were tested using a Keithley 2400 source meter. The noise current was obtained by measuring *I-t* with a Keithley 2400 source meter and then calculating it by Fast Fourier Transform (FFT).

## 2. Supplementary notes

### 2.1 Transient absorption (TA)

The transient absorption (TA) spectroscopy is a technique used to probe the time-dependent absorption profile of samples after they are excited by a pulsed laser, which is performed by a pump-probe spectrometer (Harpia, Light Conversion). Fundamental laser with a center wavelength of 1030 nm and pulse duration around 260 fs is generated at a repetition rate of 1 kHz (PHAROS-PH2, Light Conversion). Then the fundamental laser is split into two parts, one part is guided into an optical parameter amplifier (OPA, ORPHEUS-HP, Light Conversion) to create pump laser from 315 nm to 2600 nm. The frequency of pump laser is chopped at 100 KHz. The other part of laser is focused into a sapphire crystal to generate 450-1000 nm probe laser, respectively. The samples excited by the pump pulse are also sampled by the probe. The time delay ($t$) between the pump and probe may then be systematically varied to monitor the evolution of the absorption profile over time caused by the pump. A difference absorption spectrum (ΔA) is then calculated by,

$$\Delta A = log \frac{P_0}{P(t)} \tag{2.1}$$

where $P_0$ and $P(t)$ are pre-pump power and post-pump power, respectively. By changing the time delay ($t$) between the pump and the probe and recording a ΔA spectrum at each time delay, a ΔA profile as a function of the time delay ($t$) and wavelength ($\lambda$) is obtained.[1, 2]

### 2.2. Hot carrier temperature extraction from TA spectra

The high-energy tails of bleaching signal in TA spectra arises from the energy distribution of hot carriers, a feature that can be defined by a quasi-temperature $T_c$. Typically, the initial photoexcitation generates a non-equilibrium distribution of carriers. Within 100 fs, the non-equilibrium population of carriers converts into a Fermi-Dirac distribution through the carrier-carrier scattering. For carriers with excess energy far greater than the quasi-Fermi energy ($E \geq E_F$), Fermi-Dirac distribution of carriers can

be approximated by the Maxwell−Boltzmann distribution. Thus, $T_c$ can be extracted by fitting the high-energy tail using a simple Maxwell−Boltzmann distribution function

$$\Delta A(\hbar\omega) \approx -A_0(\hbar\omega)\, exp\left(-\frac{\hbar\omega}{k_B T_c}\right) \tag{2.2}$$

where $\Delta A(\hbar\omega)$ is the bleach from 2.20 eV to the lowest valley (~2.40 eV), $k_B$ is Boltzmann's constant.[3]

### 2.3. Noise assessment via time-domain signal processing and FFT

Noise of a signal is a parameter used to quantify the fluctuation degree of the signal output around its mean value. It is inherently an energy- or power-related physical quantity. The total noise power ($P_{noise}$) can be expressed as the product of the power spectral density ($PSD$) and the signal bandwidth ($\Delta f$), as shown in the following equation:

$$P_{noise} = PSD \cdot \Delta f \tag{2.3}$$

In this work, the light intensity was evaluated by the output current of the photodetector. Accordingly, the magnitude of the device noise was characterized by the current noise density ($i_{noise}$), which essentially reflects the fluctuation level of its output current. The noise power is typically related to the square of current or voltage, and therefore the power value of a current signal can be converted to the square of the current. The definition formula and dimensional unit of the noise power spectral density can be expressed as follows:

$$PSD = \frac{P_{noise}}{\Delta f} \quad [A^2\, Hz^{-1}] \tag{2.4}$$

Furthermore, we can obtain the expression for the current power spectral density as follows:

$$i_{noise} = \sqrt{PSD} \quad \left[A\, Hz^{-\frac{1}{2}}\right] \tag{2.5}$$

The practical procedure for evaluating the device noise in this work is elaborated as

follows: Firstly, the time-domain output signal of the device over a fixed duration (e.g., 100 s) was acquired. Subsequently, Fast Fourier Transform (FFT) was performed on the acquired signal to derive its power spectrum. Then, the power spectrum was divided by the bandwidth ($\Delta f = 1/T = 1/100 = 0.01\,Hz$) to obtain the PSD. Finally, the current noise density was achieved by taking the square root of the PSD.

## 3. Supporting figures

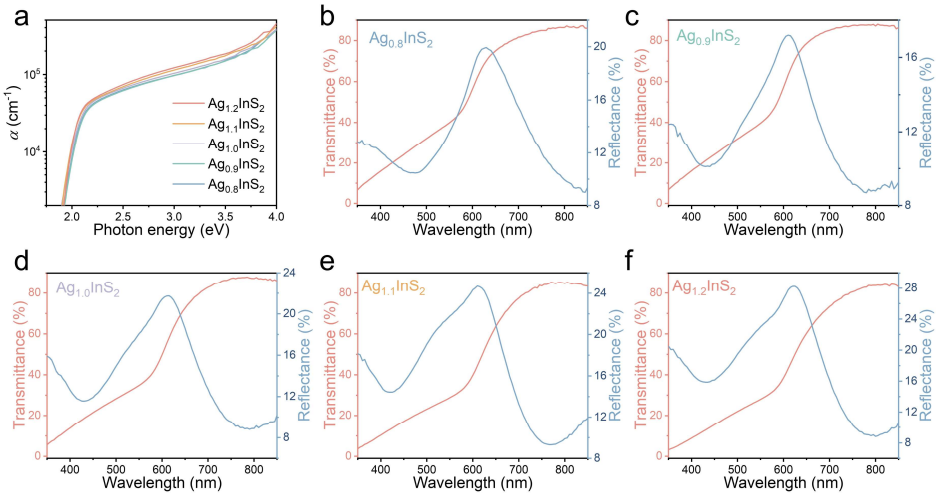


**Figure S1.** (**a**) Steady-state absorption coefficients of the $Ag_xInS_2$ thin films. Steady-state transmittance and reflectance spectra of the (**b**) $Ag_{0.8}InS_2$, (**c**) $Ag_{0.9}InS_2$, (**d**) $Ag_{1.0}InS_2$, (**e**) $Ag_{1.1}InS_2$ and (**f**) $Ag_{1.2}InS_2$ thin films.

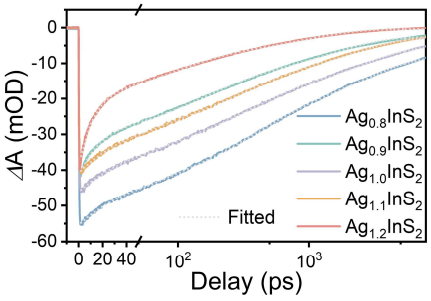


**Figure S2**. Comparison of the bleaching kinetics of all samples with a pump fluence of 10 mW. Dotted lines are fitting curves using triexponential decay.

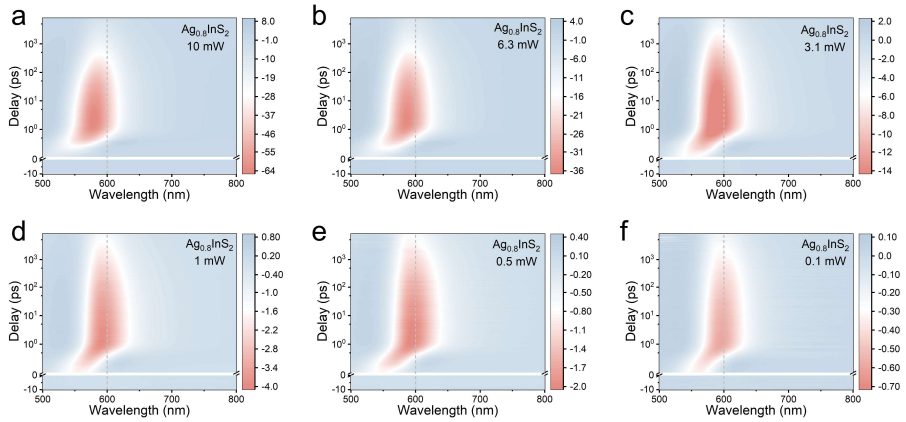


**Figure S3**. Transient transmission spectra of the $Ag_{0.8}InS_2$ sample under a pump intensity of (**a**) 10 mW, (**b**) 6.3 mW, (**c**) 3.1 mW, (**d**) 1 mW, (**e**) 0.5 mW and (**f**) 0.1 mW.

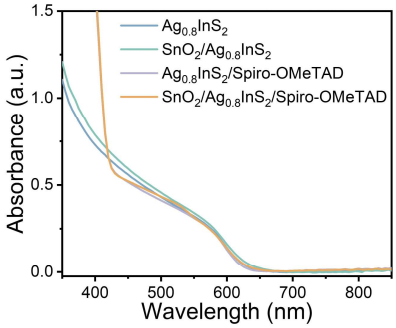


**Figure S4**. The steady-state absorbance spectra of the $Ag_{0.8}InS_2$ with different transport layers.

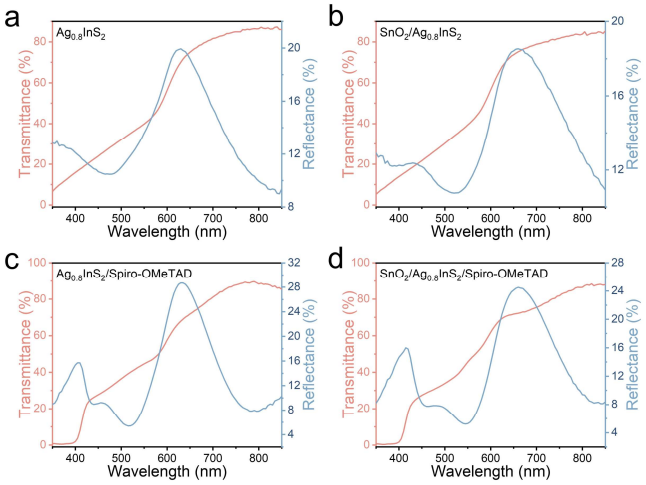


**Figure S5**. Steady-state transmittance and reflectance spectra of samples containing various transport layers.

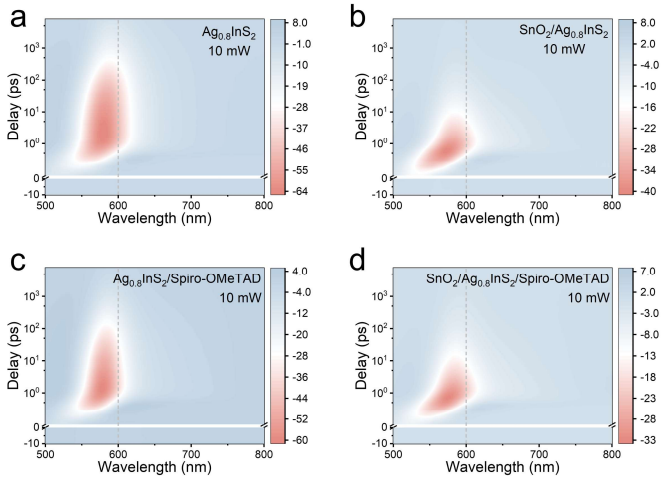


**Figure S6**. TA spectra of (**a**) $Ag_{0.8}InS_2$, (**b**) $SnO_2/Ag_{0.8}InS_2$, (**c**) $Ag_{0.8}InS_2$/Spiro-OMeTAD and (**d**) $SnO_2/Ag_{0.8}InS_2$/Spiro-OMeTAD under a pump fluence of 10 mW.

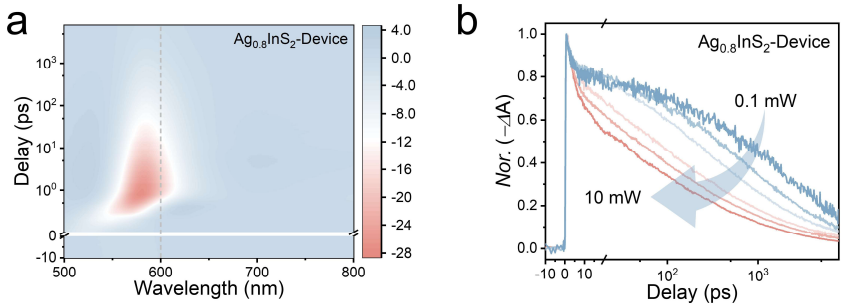


**Figure S7**. (**a**) TA spectra of the $Ag_{0.8}InS_2$ device under a pump fluence of 10 mW. (**b**) Normalized kinetics of photobleaching feature of the $Ag_{0.8}InS_2$ device.

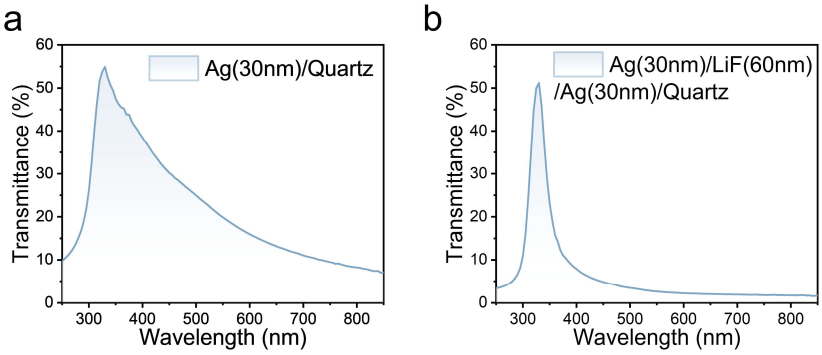


**Figure S8**. Transmittance spectra of (**a**) Ag/Quartz and (**b**) Ag/LiF/Ag/Quartz.

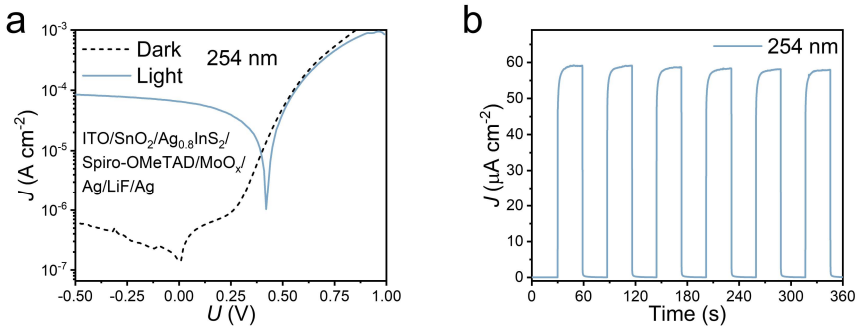


**Figure S9**. (**a**) *J-V* curve and (**b**) repeatability response of the $Ag_{0.8}InS_2$ based photodiode under 1 mW cm$^{-2}$ 254 nm ultraviolet light irradiation.

## 4. Supporting table

**Table S1.** Fitting parameters of TA kinetics in the linear response range. $R_1$, $R_2$, $R_3$ are the proportion of the three decay processes, $\tau_1$, $\tau_2$, $\tau_3$ are their lifetime constants.

| Samples | $R_1$(%) | $\tau_1$ (ps) | $R_2$(%) | $\tau_2$ (ps) | $R_3$(%) | $\tau_3$ (ps) |
|---|---|---|---|---|---|---|
| $Ag_{0.8}InS_2$ | 25.276 | 37.49373 | 38.186 | 316.16304 | 36.538 | 2504.42337 |
| $Ag_{0.9}InS_2$ | 38.128 | 13.66896 | 35.04 | 147.23353 | 26.833 | 1435.14945 |
| $Ag_{1.0}InS_2$ | 27.129 | 36.53088 | 37.634 | 281.37325 | 35.236 | 2488.43633 |
| $Ag_{1.1}InS_2$ | 34.239 | 33.91891 | 35.72 | 251.75202 | 30.041 | 1982.28585 |
| $Ag_{1.2}InS_2$ | 67.516 | 10.22152 | 20.922 | 87.90066 | 11.562 | 921.30665 |

## References


1. Berera, R.; van Grondelle, R.; Kennis, J. T. M. Ultrafast transient absorption spectroscopy: principles and application to photosynthetic systems. *Photosynth. Res.* **2009**, *101* (2-3), 105-118.
2. Cooper, J. K.; Reyes-Lillo, S. E.; Hess, L. H.; et al. Physical origins of the transient absorption spectra and dynamics in thin-film semiconductors: the case of $BiVO_4$. *J. Phys. Chem. C* **2018**, *122* (36), 20642-20652.
3. Zhang, R.; Zhou, Z.; Li, X.; et al. Low-Threshold and Ultrastable Amplified Spontaneous Emission from $CsPbBr_3$@ Glass via Glass Network Modulation. *ACS Nano* **2025**, *19* (14), 14318-14329.